

MAGNETOTORQUER-ONLY ATTITUDE CONTROL SYSTEM ROBUST TO WIDE RANGE OF INITIAL CONDITIONS FOR LOW-COST SPIN-STABILIZED ITASAT SATELLITE

Ronaldo Waschburger, ronaldo_rw@yahoo.com.br

Davi Antonio dos Santos, daviasantos@ita.br

Jacques Waldmann, jacques@ita.br

Instituto Tecnológico de Aeronáutica – Department of Systems and Control – 12228-900 – São José dos Campos, SP, Brazil

Abstract. *Air-core magnetotorquer-only attitude control system (ACS) for the low-cost, spin-stabilized ITASAT satellite is here described. ITASAT's ACS has been tested by simulation with synthetic measurement data. The proposed closed-loop ACS system is based on 3-axis attitude and angular rate estimates provided by an extended Kalman filter processing vector measurements from a Sun sensor and a 3-axis magnetometer. For improved performance, such estimates are preceded by in-flight estimation of the residual magnetometer bias. The 3-axis estimation and purely magnetic control approach circumvents the use of a passive device for nutation damping, hence aiming at rigid-body satellite dynamics that present more benevolent conditions for adequate ACS performance. The design of the nutation damping ring-aided, magnetically controlled ACS nowadays flying in the Brazilian SCD (Data Collection Satellite) satellite series was conducted under the assumption of a dedicated launch that should deploy the payload at the proper orbit, and spin-stabilized with a small initial attitude error. Moreover, magnetically-actuated attitude control systems previously described in the literature often handle first the spin axis pointing maneuver, then follows spin rate control. The ACS here described, on the other hand, can be initiated upon separation from either a 3-axis controlled launcher, or a spinning one, and simultaneously handles spin rate, spin-axis pointing, and nutation damping by activating the magnetotorquer that minimizes an asymptotic stability condition criterion. Only one magnetotorquer is active at any given time. Air-core magnetotorquers are employed for fast, accurate magnetotorquer switching to avoid nutation angle excitation when the ACS is acquiring the desired 40rpm spin rate and spin axis direction orthogonal with respect to the ecliptic plane prior to the onset of the spin-stabilized operational phase. ITASAT is a rigid body with 73.6kg, dimensions 700x700x650 mm, and principal inertia moments of 6.5 kg·m² about its principalspin-plane axes and 8.0 kg·m² about its spin axis. Its target orbit, as defined so far, is circular at 750-km altitude and a 25° inclination angle. Disturbance torques included in the simulation were those caused by gravity gradient and ITASAT's residual magnetism. Investigated here were various initial spin-axis pointing errors with respect to the desired ecliptic plane normal, and initial spin rates of 0rpm and 120 rpm, respectively corresponding to the separation from a launcher's 3-axis controlled last stage and from a launching vehicle with a spin-stabilized last stage – such as the Brazilian-made VLS (Satellite Launch Vehicle). The simulation results have indicated that proper attitude acquisition occurred in both orbit injection conditions. Injection by a 3-axis controlled launcher called for about 5 days of ACS maneuvering, when the angular momentum pointing error magnitude remained under 3° and spin rate error to 1rpm, whereas steady-state nutation angle remained below ±2°.*

Keywords: Satellite; Attitude Dynamics, Extended Kalman Filter, Spin Stabilization, Nonlinear Control

1. INTRODUCTION

Low-cost satellites often employ a 3-axis magnetometer and Sun sensors for attitude determination and magnetotorquers for attitude control (Azor *et al.*, 2001). Instances of such an approach are found in Krogh (2002), Svartveit (2003), and Wisniewski (2000). ITASAT is intended to be an university-designed, spin-stabilized satellite weighing about 74kg and 700x700x650 mm in size. ITASAT is not equipped with actuators for orbit control. Its 3-axis attitude determination system (SDA), based on the extended Kalman filter processing vector measurements from on-board magnetometer and Sun sensors for attitude quaternion estimation, is described in detail in Santos (2008) and Santos and Waldmann (2009). A closed-loop, autonomous, attitude control system is proposed to operate on 3-axis attitude and angular rate estimates to drive the on-board magnetotorquers with the purpose of precessing the angular momentum vector to acquire and maintain the desired attitude and spin rate, and concurrently damping the undesired nutation.

ITASAT's main purpose is to relay meteorological data transmitted from field stations spread over the Brazilian territory to specific ground antennas for further processing and weather forecast. ITASAT's attitude control has been inspired by INPE's design of Data Collecting Satellites SCD-1 and SCD-2 (Carrara *et al.*, 1994; Kuga *et al.*, 1999), wherein telemetry data from the on-board 3-axis magnetometer and Sun sensors are received and processed at mission control station on the ground. Estimates of spin-axis attitude, spin rate as well in the case of SCD-2, and control signals are then computed and attitude is numerically propagated (Zanardi and Lopes, 2000) for the next 90 days. Telecommands with respective time tags are then issued from the ground upwards to the on-board computer via an uplink to drive the magnetotorquers, whose magnetic dipoles' interaction with the geomagnetic field gives rise to torques that precess the angular momentum vector towards the desired direction and magnitude. Thus the

magnetotorquers can be activated even when the satellite is in a position in its orbit such that the communications link with mission control is off range. SCD's injection in the desired orbit was known beforehand to be performed by a dedicated launch vehicle with a spinning last stage, which would deploy the satellite in a close vicinity of the correct spin-axis attitude (Orlando, 1999); hence a ring partially filled with silicone oil was employed for nutation damping (Lopes *et al.*, 1986; Lopes, 1987).

On the other hand, low-cost ITASAT is expected to ride piggyback onto some thus far indefinite, paid-for, primary payload in an as yet unknown launcher. Often the last stage of commercially available launchers is 3-axis controlled, and does not present a spinning capability. It is thus quite likely that ITASAT may be injected into an as yet unknown orbit with a significantly incorrect initial attitude from the point of view of thermal safety, suffering from reduced solar panel irradiation for battery charging, and deprived of sufficient angular *momentum* for adequate spin-stabilization. Such initial conditions may lead to a tumbling motion. Hence the need for autonomous 3-axis attitude and angular rate vector estimation and control, without need for interference from mission control station, and robustness to initial conditions quite apart from the desired spin-axis attitude and spin rate. Because modeling the complex fluid dynamics and sloshing in the nutation damping ring when subject to tumbling is quite involved (Alfriend, 1974; Fonseca *et al.*, 1990; Changsheng, 2001; Vreeburg, 2005), ITASAT has been assumed to be a rigid body. Therefore, ITASAT's attitude control system (ACS) should provide control torques that precess the angular *momentum* to acquire the correct spin-axis attitude and spin rate, in addition to damping nutation.

The technological innovations proposed here with respect to the implementation in SCD-2, namely, autonomous control and purely magnetic actuation in ITASAT, are evidence, respectively, of the undergoing technological drive forward in the Brazilian aerospace scenario, and the need to fulfill ITASAT's mission under the uncertainties regarding the means that will be used for launch and injection into orbit. Most certainly, modifications and simplifications to the present proposal should be considered when devising an ACS to match its on-board implementation with the available memory and throughput in ITASAT's on-board computer.

Previous work on spin-stabilized, purely magnetic satellite control by Shigehara (1972) utilized magnetotorquers aligned with the spin axis and in the spin plane, respectively, to separately control spin-axis attitude and spin rate assuming known attitude and angular rate. Kuga *et al.* (1987) confirmed by simulation the potential of magnetic actuation for the SCD's along with nutation damping rings. Quarter-Orbit Magnetic Attitude Control for SCD-2 was reported by Orlando *et al.* (1998). The formulation and Lyapunov-based proof of convergence of a linearized control law operating on quaternion and angular rate disturbances about the operating conditions in a 3-axis stabilized satellite is found in Wang *et al.* (1998). Purely magnetic nutation damping with Lyapunov-based proof of convergence for spin stabilization, even about the principal axis of smallest inertia, has been described by Holden (1999). Santoni (2000) proposed an extended Kalman filter for spin-axis attitude estimation from Sun sensor and geomagnetic field vector measurements, and purely magnetic actuation to control the spin-axis attitude, spin rate, and nutation damping.

The paper is structured as follows. Next section presents the problem formulation, satellite attitude kinematics and angular rate dynamics, and the modeling of the operation environment for the ACS on-board requirements and ground-truth generation to simulate the measurement vectors. Then the magnetic control law that maximizes the rate of decay of the angular *momentum* pointing error quadratic norm is described, followed by simulation results and conclusions.

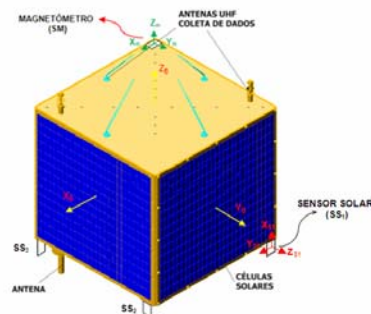


Figura 1. ITASAT's present configuration and available sensor suite.

2. MAGNETIC ACTUATION, ATTITUDE, ORBIT, AND ENVIRONMENT MODELING

The present approach to rigid-body, low-cost, spin-stabilized ITASAT's ACS investigates the use of air-core magnetotorquers for purely magnetic attitude control and nutation damping in closed loop with the SDA based on an extended Kalman filter for attitude and angular rate vector estimation from vector measurements of the Sun direction and the geomagnetic field (Santos, 2008; Santos and Waldmann, 2009).

ITASAT is modeled as a rigid-body, spin-stabilized satellite to operate in a circular, low-Earth orbit with 25° inclination. Air-core magnetotorquers (MTQ) are the only means to acquire the desired spin-axis attitude and spin rate, and damping the nutation motion that might arise during the maneuvers to precess the angular *momentum* vector. The

relevant disturbing torques that affect attitude when operating in a low orbit are those induced by eddy currents and gravity gradient. Joint attitude and angular rate estimates are available for the magnetic control law from the extended Kalman filter AVEKF in ITASAT's SDA, which comprises magnetometer bias estimation for improved accuracy. The estimation AVEKF that employs vector measurements provided by Sun sensors and 3-axis magnetometer is described in detail elsewhere (Santos 2008; Santos and Waldmann, 2009).

Figure 1 shows the location of the solar panels that provide energy for the satellite's various subsystems and battery recharging. Spin axis k_B is aligned with the principal axis of largest inertia Z_B . Thus, one attitude constraint is that the desired spin-axis attitude should be as close as possible to orthogonal with respect to the direction of the Sun to maximize irradiation. However, as shown in Figure 2, there are infinitely many distinct attitudes that are consistent with the above constraint. Only one obviates the need for recurrent spin-axis maneuvering due to Earth's translation in its orbit around the Sun though. That is when spin axis k_B , while orthogonal with respect to the direction of the Sun, simultaneously remains perpendicular to the ecliptic plane (Orlando *et al.*, 1998). To protect its lower and upper panels from irradiation and thus secure the satellite's thermal safety, the solar angle – defined from spin-axis and the direction of the Sun – should be maintained in the range from 80° e 100° (Kuga *et al.*, 1999). Hence, ITASAT's spin-axis k_B should be restricted to move within a 10° cone about the ecliptic plane normal. Desired spin rate is 40rpm.

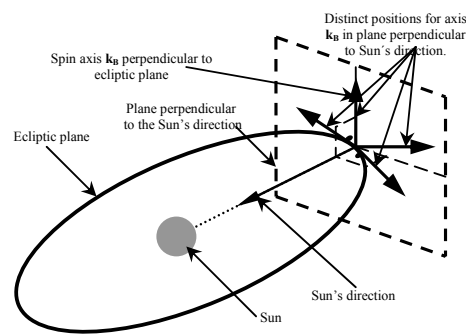


Figure 2. Ecliptic plane and attitude constraint plane orthogonal to the direction of the Sun.

Cartesian coordinate frames for describing the satellite attitude and motion along its orbit are depicted in Figure 3 and Figure 4:

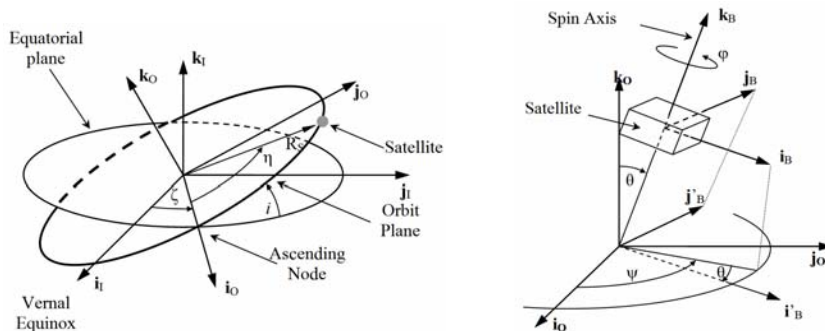


Figure 3. Inertial S_I , orbital S_O , and body S_B Cartesian coordinate frames (Shigehara, 1972).

where R_S is the position vector from the Earth's center to the satellite's center; η , the angular position of the satellite along its orbit (true anomaly since the orbit is circular) with respect to the ascending node; ζ , the right ascension of the ascending node; and i , the orbit inclination. Inertial axis i_I points to vernal equinox whereas k_I is orthogonal to the equatorial plane. Regarding the orbital frame, i_O points to the ascending node and k_O is perpendicular to the orbit plane. Finally, the attitude Euler angles used in the problem formulation are defined by the rotation sequence: ψ (azimuth) about k_O , θ (elevation) about j'_B , and ϕ (spin) about k_B .

In spite of the desired pure spin ω_{spin} about the principal axis of largest inertia k_B , nutation may be excited by the action of external torques, either disturbances, or the control torque aiming at precessing the angular momentum H into alignment with the normal to the ecliptic plane, as depicted in Figure 4. Nutation is characterized by an angular rate component in the spin plane orthogonal to the spin axis, thus yielding the undesired misalignment between k_B and H known as the nutation angle. As a result, k_B wobbles and spin axis pointing accuracy degrades. The ACS should precess H with respect to the inertial reference frame while concurrently damping the nutation angle with control torques arising from the interaction of magnetotorquer magnetic dipole with the geomagnetic field.

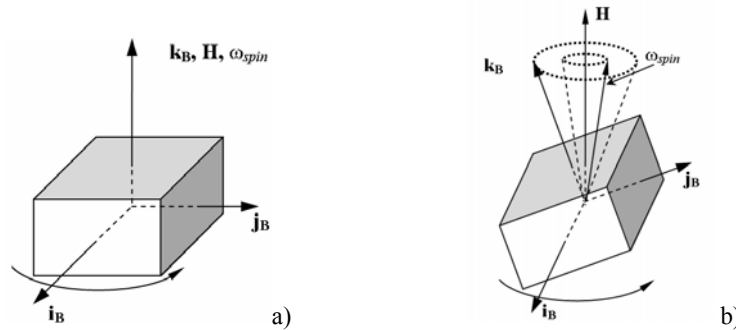


Figure 4. Rotational motion: pure spin in a); combined spin and nutation in b).

Rigid body equations of motion are as follows, with ω the angular rate vector of the body relative to the inertial frame, I and I_S the inertia moment about principal axes i_B, j_B in the spin plane and the largest inertia moment about k_B , respectively, and T the external torque vector:

$$\begin{aligned}\dot{\omega}_i &= I^{-1} ((I - I_S)\omega_j\omega_k + T_i) \\ \dot{\omega}_j &= I^{-1} ((I_S - I)\omega_i\omega_k + T_j) \\ \dot{\omega}_k &= I_S^{-1} T_k\end{aligned}\quad (1)$$

Attitude parameterization employs the quaternion q to circumvent singularities and for improved numerical accuracy in comparison with Euler angles. Use of benchmark analytical solutions to evaluate numerical integration algorithms for attitude propagation so that distortions in the solution are due to artifacts introduced by the particular implementation of finite accuracy mathematics in the algorithm can be found in Markley (2008) and Zanardi and Lopes (2000). The analytical solution by Poincot (Wiesel, 1997) of a rigid, rotating rotor free of external torques and without energy dissipation yields a constant nutation angle. This has been used as a benchmark to select a convenient numerical integration algorithm for attitude propagation, the 4th-order Runge-Kutta *ode45* available in Matlab's Simulink environment, with the maximum integration step set to 0.05s and relative tolerance 10^{-6} (Waschburger *et al.*, 2008a). Attitude kinematics is thus described as follows, where λ is a scalar; q_1 relates to unit vector i_B ; q_2 to j_B ; and q_3 to k_B :

$$\dot{q} = \begin{bmatrix} \dot{\lambda} \\ \dot{q}_1 \\ \dot{q}_2 \\ \dot{q}_3 \end{bmatrix} = \frac{1}{2} \begin{bmatrix} 0 & -\omega_i & -\omega_j & -\omega_k \\ \omega_i & 0 & \omega_k & -\omega_j \\ \omega_j & -\omega_k & 0 & \omega_i \\ \omega_k & \omega_j & -\omega_i & 0 \end{bmatrix} \begin{bmatrix} \lambda \\ q_1 \\ q_2 \\ q_3 \end{bmatrix}\quad (2)$$

Satellite attitude Euler angles are retrieved from the attitude quaternion as follows. Consider the direction cosine matrices DCM_B^1 that transforms a vector representation from S_1 to another in S_B , DCM_B^0 from S_0 to S_B , and DCM_1^0 from S_0 to S_1 . Then $DCM_B^0 = DCM_B^1 DCM_1^0$ where:

$$DCM_B^1 = \begin{bmatrix} \lambda^2 + q_1^2 - q_2^2 - q_3^2 & 2(q_1q_2 + \lambda q_3) & 2(q_1q_3 - \lambda q_2) \\ 2(q_1q_2 - \lambda q_3) & \lambda^2 - q_1^2 + q_2^2 - q_3^2 & 2(q_2q_3 + \lambda q_1) \\ 2(q_1q_3 + \lambda q_2) & 2(q_2q_3 - \lambda q_1) & \lambda^2 - q_1^2 - q_2^2 + q_3^2 \end{bmatrix}$$

$$DCM_B^0 = \begin{bmatrix} \cos\psi \cos\theta \cos\varphi - \sin\psi \sin\varphi & \sin\psi \cos\theta \cos\varphi + \cos\psi \sin\varphi & -\sin\theta \cos\varphi \\ -\cos\psi \cos\theta \sin\varphi - \sin\psi \cos\varphi & -\sin\psi \cos\theta \sin\varphi + \cos\psi \cos\varphi & \sin\theta \sin\varphi \\ \cos\psi \sin\theta & \sin\psi \sin\theta & \cos\theta \end{bmatrix}$$

$$DCM_1^0 = \begin{bmatrix} \cos\zeta & -\cos i \sin\zeta & \sin i \sin\zeta \\ \sin\zeta & \cos i \cos\zeta & -\sin i \cos\zeta \\ 0 & \sin i & \cos i \end{bmatrix}$$

and use of the inverse tangent function $atan2()$ yields the desired Euler angles where i and j in $DCM(i,j)$ are the i -th line and j -th column, respectively:

$$\begin{aligned}\psi &= a \tan 2(\sin \psi \sin \theta, \cos \psi \sin \theta) = a \tan 2(DCM_B^0(3,2), DCM_B^0(3,1)) \\ \theta &= a \cos(\cos \theta) = a \cos(DCM_B^0(3,3)) \\ \varphi &= a \tan 2(\sin \theta \sin \varphi, \sin \theta \cos \varphi) = a \tan 2(DCM_B^0(2,3), -DCM_B^0(1,3))\end{aligned}\quad (3)$$

Magnetic control torque T_{Mag} results from the interaction between magnetotorquer magnetic dipole M and geomagnetic field B ; eddy currents generate a disturbance torque T_{eddy} whose coefficient k_e depends on satellite

geometry and conductivity; and the gravity gradient yields the disturbance torque T_{GG} due to the varying gravitational pull at different parts of the satellite (Wertz, 1978):

$$\mathbf{T}_{Mag} = \mathbf{M} \times \mathbf{B} \quad \mathbf{T}_{eddy} = k_c (\boldsymbol{\omega} \times \mathbf{B}) \times \mathbf{B} \quad \mathbf{T}_{GG} = (3\mu / \|\mathbf{R}_s\|^3) [\hat{\mathbf{R}}_s \times (\mathbf{J} \cdot \hat{\mathbf{R}}_s)] \quad (4)$$

where \mathbf{J} is the satellite inertia tensor; μ the Earth's gravitation constant; and $\hat{\mathbf{R}}_s$ a unit vector along \mathbf{R}_s . The geomagnetic field \mathbf{B} has been modeled with World Magnetic Model WMM-2005 (McLean *et al.*, 2004), 12th order for the ground truth model and 4th order for the on-board model needed for attitude estimation by SDA (Santos, 2008; Santos and Waldmann, 2009). Actual satellite motion is modeled by the Simplified General Perturbations Satellite Orbit Model 4 (SPG4) (Vallado *et al.*, 2006) for ACS simulation and performance evaluation, and the on-board SDA utilizes a Keplerian orbit model that takes into consideration the J_2 disturbance caused by the Earth's oblateness giving rise to the regression of the ascending node. The SPG4 model is valid for low-Earth orbits such as ITASAT's. Parameters in the latter model can be updated by the uplink from mission control station on the ground to the satellite.

A thorough description of the 3-axis magnetometer and Sun sensor models, the extended Kalman filter MAGEKF for magnetometer bias estimation, the AVEKF for joint quaternion and angular rate estimation, and the attained SDA performance are found in Santos (2008) and Santos and Waldmann (2009).

Air-core magnetotorquers (MTQ's) are positioned along $\mathbf{k}_B, \mathbf{i}_B, \mathbf{j}_B$, and can be switched on to provide a known, fixed magnetic dipole magnitude $|\mathbf{M}|$ with a commanded polarity, one MTQ at a time, or off. MTQ actuation disturbs magnetometer readings. Satellite tumbling makes it difficult to estimate magnetometer bias under the influence of MTQ actuation in comparison with pure spin. Thus, magnetometer reading occurs solely when MTQ's are disabled. MTQ's are disabled during 20% of the 0.1s duty cycle shown in Fig. 5.

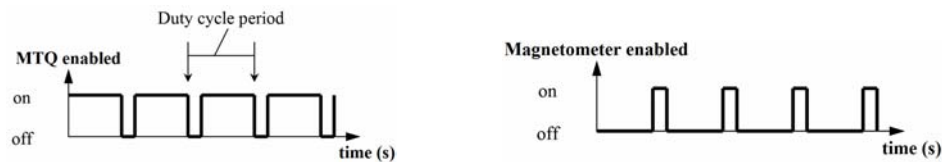


Figure 5. Enabled magnetotorquer and magnetometer duty cycles.

Furthermore, MTQ's are enabled or disabled according to the following rules:

- MTQ's are disabled when the angular pointing error E_{ap} , defined as the angle between the desired angular momentum \mathbf{H}_{ref} and satellite angular momentum \mathbf{H} , goes below 0.25° , AND the spin rate error magnitude is under 0.25% of its nominal value;
- MTQ's are enabled when E_{ap} is beyond 0.5° , OR the spin rate error magnitude is over 0.5% of its nominal value;
- MTQ's are disabled whenever the joint attitude and angular rate vector extended Kalman filter AVEKF estimator in the SDA diverges (Santos, 2008);
- MTQ's are disabled when the satellite undergoes the eclipse in every 100-minute orbit period, a condition found to compromise severely the accuracy of attitude estimates to a point that ACS should not be engaged (Santos, 2008; Santos and Waldmann, 2009).

SDA divergence is flagged when the trace of the estimation error covariance error matrix \mathbf{P} is above the $5 \cdot 10^{-4}$ threshold found by simulation. Criteria should be established to reinitialize the filter in case divergence lasts too long, or the trace of covariance \mathbf{P} becomes too large. Santos (2008) and Santos and Waldmann (2009) details the MAGEKF and AVEKF algorithms and SDA performance under tumbling, slow motion, and spinning with eclipse.

3. MAXIMUM ANGULAR MOMENTUM ERROR NORM REDUCTION RATE CONTROL LAW

ITASAT's ACS operation is based on the asymptotic stability proof reported in Shigehara (1972) and employed by Orlando *et al.* (1998). MTQ actuation always reduces the norm of the angular momentum error vector $\mathbf{E} = E \hat{\mathbf{E}} = \mathbf{H}_{ref} - \mathbf{H}$ between the reference angular momentum and the satellite's, subject to at most one MTQ energized at any moment in time. The latter is due to unknown electromagnetic interaction among the MTQ's and has been employed in both Shigehara (1972) and Orlando *et al.* (1998). However, both separate the magnetic actuation: first spin-axis attitude control, then follows spin rate control. Notice that the SCD-2's ACS was devised assuming injection in orbit in a close vicinity of the desired spin-axis attitude and spin rate. Distinctly, the proposal for ITASAT's ACS is to engage the MTQ that maximizes the rate of decay of the angular momentum error norm $d(\mathbf{E} \cdot \mathbf{E})/dt < 0$ without any regard for whether the action yields spin-axis precession towards the desired pointing or spin rate control. The derivation follows Shigehara's (1972) notation:

$$\mathbf{H} = I \omega_i \mathbf{i}_B + I \omega_j \mathbf{j}_B + I_S \omega_k \mathbf{k}_B \quad \text{and} \quad \mathbf{H}_{ref} = I_S \omega_{ref} \mathbf{k}_{ref} \quad (5)$$

$$\mathbf{E} = E \hat{\mathbf{E}} = \mathbf{H}_{\text{ref}} - \mathbf{H} \text{ where } \|\hat{\mathbf{E}}\| = 1 \quad (6)$$

A sufficient condition to assure asymptotic stability is the inequality:

$$\frac{1}{2} \frac{d(\mathbf{E} \cdot \mathbf{E})}{dt} = \frac{1}{2} \left(\frac{d(\mathbf{E})}{dt} \cdot \mathbf{E} + \mathbf{E} \cdot \frac{d(\mathbf{E})}{dt} \right) = \mathbf{E} \cdot \frac{d(\mathbf{E})}{dt} < 0 \quad (7)$$

where

$$\frac{d(\mathbf{E})}{dt} = \dot{\mathbf{H}}_{\text{ref}} - \dot{\mathbf{H}} = \mathbf{0} - (\mathbf{T} + \mathbf{T}_{\text{Pert}}) \quad (8)$$

The vector time derivatives are computed from the perspective of an inertial observer. $\mathbf{T} = \mathbf{T}_{\text{Mag}}$ and \mathbf{T}_{Pert} are control and disturbance torques, respectively. Substituting the above in the sufficient condition for asymptotic stability:

$$\mathbf{E} \frac{d(\mathbf{E})}{dt} = -\mathbf{E} \cdot (\mathbf{T}_{\text{Mag}} + \mathbf{T}_{\text{Pert}}) = -\mathbf{E} \cdot (\mathbf{M} \times \mathbf{B}) - \mathbf{E} \cdot \mathbf{T}_{\text{Pert}} < 0 \quad (9)$$

Since the disturbance torque \mathbf{T}_{Pert} is expected to have a magnitude far smaller than \mathbf{T}_{Mag} , the above inequality is approximated to:

$$\mathbf{E} \cdot (\mathbf{M} \times \mathbf{B}) > 0 \quad (10)$$

Recalling that only one MTQ can be active at a given moment in time, and taking into consideration the magnetic dipoles that can be generated with the adequate polarity at each MTQ aligned with \mathbf{S}_B axes \mathbf{i}_B , \mathbf{j}_B , \mathbf{k}_B , respectively, the above condition can be stated component-wise as:

$$\begin{aligned} \alpha \text{ sign}(\mathbf{E} \cdot (\mathbf{i}_B \times \mathbf{B})) > 0 & \text{ in case the } \mathbf{i}_B\text{-MTQ is engaged; or} \\ \beta \text{ sign}(\mathbf{E} \cdot (\mathbf{j}_B \times \mathbf{B})) > 0 & \text{ in case the } \mathbf{j}_B\text{-MTQ is engaged; or} \\ \gamma \text{ sign}(\mathbf{E} \cdot (\mathbf{k}_B \times \mathbf{B})) > 0 & \text{ in case the } \mathbf{k}_B\text{-MTQ is engaged;} \end{aligned} \quad (11)$$

where $\alpha > 0$ is the maximum magnetic dipole magnitude that can be produced by the \mathbf{i}_B -MTQ, and likewise $\beta > 0$ with respect to the \mathbf{j}_B -MTQ, and $\gamma > 0$ to the \mathbf{k}_B -MTQ. Since all MTQ's have the same nominal magnetic dipole, one assumes $\alpha = \beta = \gamma$ and the maximizing MTQ is the one aligned with axis \mathbf{s}^* such that:

$$\mathbf{s}^* = \arg \max_{\mathbf{s} \in \{\mathbf{i}, \mathbf{j}, \mathbf{k}\}} |\mathbf{E} \cdot (\mathbf{s}_B \times \mathbf{B})| \quad (12)$$

The correct polarity of the maximizing MTQ is selected to comply with the respective inequality in Eq. (11). Consequently, comparing with Eq. (7) one notices that the above control law yields a maximum rate of decay $|d(\mathbf{E} \cdot \mathbf{E})/dt|$ in the quadratic angular momentum error (Waschburger and Waldmann, 2008b).

4. SIMULATION AND RESULTS

Table 1 describes ITASAT's parameters and nominal orbit, SDA initialization values (Santos and Waldmann, 2009), and other relevant constants for the simulation. Remaining constants are found in WGS-84. Two cases have been investigated: Case I is when ITASAT is injected in orbit with an initial spin rate of 120rpm to mirror SCD-2's initial condition (Orlando *et al.*, 1998), and Case II with zero rpm as in Krogh (2002). ACS performance has been evaluated during initial maneuvers and in steady state in terms of angular momentum pointing error, nutation angle, and solar angle. The latter is defined as the angle between spin axis \mathbf{k}_B and the direction of the Sun. Furthermore, spin-axis pointing and spin rate settling times were also determined. Though ITASAT's attitude estimation and control cycle is to operate at 10Hz according to the 0.1s duty cycle in Fig. (5), simulation results were stored every 10s to save memory space.

Both Cases I and II have been investigated with the four possible combinations, named Subcases, of $\pm 15^\circ$ initial pointing error in ψ and θ , each Subcase encompassing four realizations. The heavy computational load precluded the statistical analysis of ACS performance with Monte Carlo simulation. Angular momentum pointing error E_{ap} , nutation angle θ_{Nut} , and spin-axis pointing errors are given by:

$$E_{ap} = \arccos\left(\frac{\langle \mathbf{H}_{ref}, \mathbf{H} \rangle}{\|\mathbf{H}_{ref}\| \cdot \|\mathbf{H}\|}\right) \quad \theta_{Nut} = \arccos\left(\frac{\mathbf{H}_{kB}}{\|\mathbf{H}\|}\right) \quad (13)$$

$$E_{\psi} = \psi_{ref} - \psi \quad E_{\theta} = \theta_{ref} - \theta \quad (14)$$

Table 1. Simulation parameters.

Principal inertia, spin plane.	I	6,5	kg·m ²	On-board ⁽¹⁾ .
Principal inertia, spin axis.	I _S	8,0	kg·m ²	On-board ⁽¹⁾ .
Inertia tensor.	J	$\begin{bmatrix} 6,5080 & -0,0080 & -0,0080 \\ -0,0080 & 6,4920 & 0,0080 \\ -0,0080 & 0,0080 & 8,0080 \end{bmatrix}$	kg·m ²	Ground-truth ⁽²⁾ .
Nominal spin rate.	ω_{ref}	40	rpm	
MTQ magnetic dipoles.	α, β, γ	10	A·m ²	On-board ⁽¹⁾⁽⁴⁾ .
	$\alpha_{true}, \gamma_{true}$	11	A·m ²	Ground-truth ⁽²⁾⁽⁴⁾ .
	β_{true}	9		
Eddy current torque decay coeff.	k_e	500	Ω/m^4	(Wertz, 1978)
Orbit inclination.	i	25	degrees	
Orbit altitude.	h	750	km	
Initial true anomaly measured from ascending node.	η_0	0	degrees	
Initial right ascension of ascending node.	ζ_0	320	degrees	
Orbit excentricity.	e	0	–	On-board ⁽¹⁾ .
	e_{true}	0,001	–	Ground-truth ⁽²⁾ .
Atmospheric drag coefficient.	B_{drag}	$1,682 \cdot 10^{-5}$	–	SCD1.
Initial ψ and θ spin-axis pointing error magnitude. ⁽³⁾	–	15	degrees	
Launch date	Date	2009, 01 (month), 01 (day), 00h:00min:00sec.		
Measurement error covariance matrix.	R	$\begin{bmatrix} \mathbf{R}_1 & \mathbf{0}_{3 \times 3} \\ \mathbf{0}_{3 \times 3} & \mathbf{R}_2 \end{bmatrix}$	T ²	R ₁ ⁽⁵⁾ R ₂
Modeling error power spectral density matrix.	Q	$10^{-6} \begin{bmatrix} \mathbf{Q}_1 & \mathbf{0}_{4 \times 3} \\ \mathbf{0}_{3 \times 4} & \mathbf{Q}_2 \end{bmatrix}$	1/s rad ² /s ³	Q ₁ ⁽⁶⁾ Q ₂
Initial AVEKF state.	$\hat{\mathbf{x}}_{0 0}^*$	[.9728, .2017, .0232, .1118, 0, 0, 40.2π/60] ^T	– rad/s	
Initial AVEKF estimation error covariance matrix.	P _{0 0} [*]	$\begin{bmatrix} \mathbf{P}_1 & \mathbf{0}_{4 \times 3} \\ \mathbf{0}_{3 \times 4} & \mathbf{P}_2 \end{bmatrix}$	– (rad/s) ²	P ₁ ⁽⁷⁾ P ₂
Ground-truth initial angular velocity about i _B , j _B , k _B .	ω_0	[5.7·π/180, 5.7·π/180, 120·2π/60] ^T	rad/s	Case I.
	ω_0	$\mathbf{0}_{3 \times 1}$	rad/s	Case II.

⁽¹⁾ Parameters for use on board are applied to simplified models in SDA and ACS; Keplerian orbit model assumed updated every 10 orbits by upload from mission control via communications uplink.

⁽²⁾ Ground-truth parameters are for more elaborate models that better represent the actual system dynamics.

⁽³⁾ Initial pointing directions investigated in each Case are the four possible combinations in ψ and θ errors.

⁽⁴⁾ MTQ's can be engaged during 80% of 0.1s duty-cycle; air-core MTQ dynamics have been neglected.

⁽⁵⁾ $\mathbf{R}_1 = 4 \cdot 10^{-14} \mathbf{I}_3$ in Tesla² units (T²) refers to magnetometer measurements, and $\mathbf{R}_2 = (0.5 \cdot \pi/180)^2 \cdot \mathbf{\Pi} \cdot \mathbf{I}_2 \cdot \mathbf{\Pi}^T + 10^{-6} \mathbf{I}_3$ with

$$\mathbf{\Pi} = \begin{bmatrix} -\sin(S_{\varphi})\sin(S_{\theta}) & \cos(S_{\varphi})\cos(S_{\theta}) \\ -\sin(S_{\varphi})\cos(S_{\theta}) & -\cos(S_{\varphi})\sin(S_{\theta}) \\ \cos(S_{\varphi}) & 0 \end{bmatrix}$$

and S_ψ , S_θ are, respectively, azimuth and elevation [rad] of the Sun's direction relative to the Sun sensor frame aligned with S_B (Santos, 2008; Waldmann and Santos, 2009).

⁽⁶⁾ $\mathbf{Q}_1 = 8 \cdot \mathbf{I}_4$ and $\mathbf{Q}_2 = 20 \cdot \mathbf{I}_3$ rad²/s.

⁽⁷⁾ $\mathbf{P}_1 = 0.1 \cdot \mathbf{I}_4$ and $\mathbf{P}_2 = (\pi/180)^2 \cdot \mathbf{I}_3$ (rad/s)².

Figures 6 and 7 show realizations of Case II. Table 2 provides a comparison of worst-case results for Cases I and II.

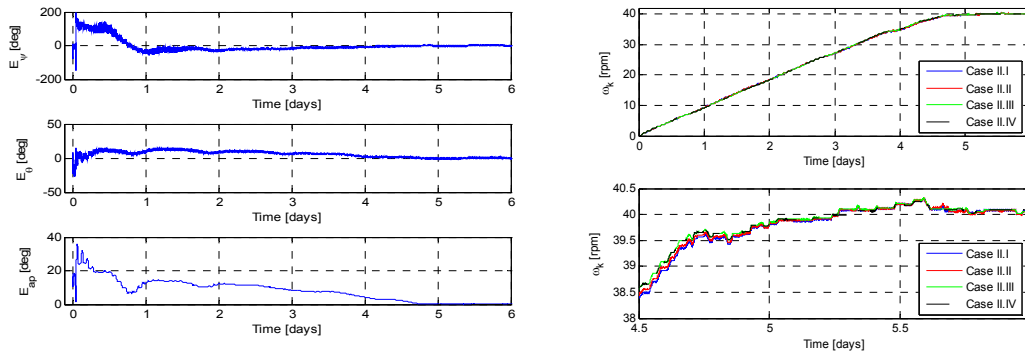


Figure 6. Case II realization. Left: spin-axis and angular momentum pointing errors, and right: spin rate acquisition.

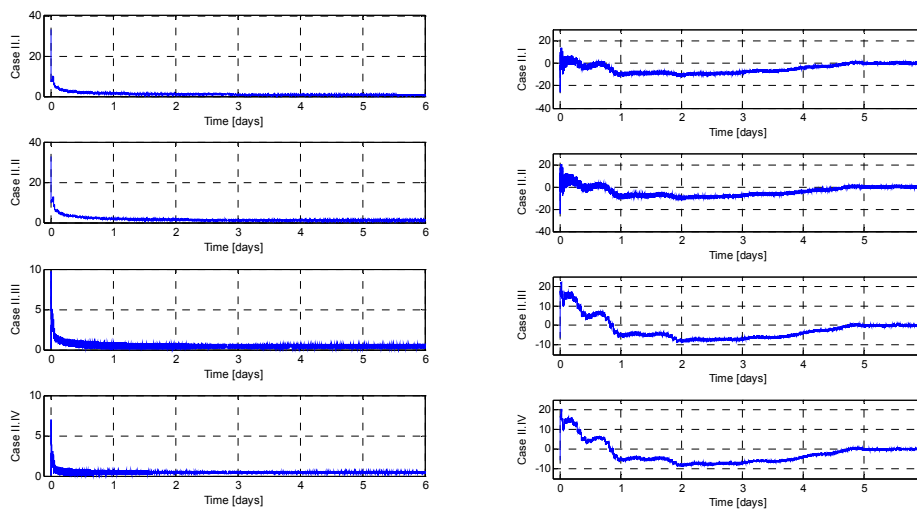


Figure 7. Case II: 4 realizations. Left: Nutation angle [deg], and right: 90-degree-complement solar angle [deg].

In Case I, orbit injection when spinning at 120rpm, E_{ap} was always below 20°, and it took 9 days in the worst case to consistently comply with the 10° cone constraint. Settling time was 10 days to reach a pointing accuracy of 2.5°. Spin rate was reduced to 41rpm after 10 days, with a steady-state error of 0.5rpm. Nutation angle θ_{Nut} always remained under 1.5°. Instead of the solar angle, Table 2 displays its 90°-complement, that is, the angle between the spin plane and the Sun's direction. The latter reached a 16° peak value, remained above the 10° cone constraint for about 9 days, and varied within $\pm 2^\circ$ in steady-state. Notice that for the SCD-2's ACS and its predicted acquisition maneuvers in its first year of operation reported in Carrara and Guedes (1994), a simulation-based performance investigation indicated a far more serious constraint violation: trespassing the 10° cone constraint for up to 200 days, and reaching a peak value of 50°, that is, a peak solar angle of 40° at about the 40th day past injection into orbit.

In Case II, orbit injection without spin, E_{ap} was always below 45°, and it took only 3 days in the worst case to consistently comply with the 10° cone constraint. Settling time was 5 days to reach a pointing accuracy of 2.5°. Spin rate was produced, reaching 39rpm after about 5 days, with a steady-state error of 0.5rpm. Nutation angle θ_{Nut} underwent a peak value of 40° during the initial phase of acquisition maneuvers due to the initial absence of angular rate, and the early arising of of an angular rate component in the spin plane. However, as the angular momentum evolved and its magnitude raised, θ_{Nut} was significantly reduced and converged to about 1.5°. The 90°-complement of the solar angle presented a worst-case peak of 25°, violated the 10° cone constraint for about 3 days, and reached steady state within a $\pm 2^\circ$ error.

Table 1. Simulation results.

Variable	Case I	Case II	Units
Peak E_{ap} during maneuver.	20	45	degrees
Steady-state E_{ap} limit.	2.5	2.5	degrees
Time to remain within 10° cone constrain, worst case.	9	3	days
Spin-axis pointing error settling time to reach 3° -accuracy.	10	5	days
Steady-state spin rate error magnitude.	0.5	0.5	rpm
Spin rate error settling time.	10	5	days
Peak θ_{Nut} during maneuver.	1.5	40	degrees
Steady-state θ_{Nut} .	1.5	1.5	degrees
Peak 90° -complement solar angle during maneuver.	16	25	degrees
Time to remain within 10° cone constrain with respect to the 90° -complement solar angle, worst case.	9	3	days
Steady-state 90° -complement solar angle.	± 2	± 2	degrees

5. CONCLUSIONS

In both Cases *I* and *II*, the proposed ACS for ITASAT showed its effectiveness acquiring and maintaining the desired spin-axis attitude and spin rate. Injection when spinning at 120rpm , as in Case *I*, produced a smaller peak angular momentum error, nutation angle, and 90° -complement solar angle. However, maneuvering time to reach a 3° -pointing error accuracy with respect to the ecliptic plane normal called for 10 days in Case *I*, in a sharp contrast to the 5 days in Case *II*, that is injection from a 3-axis controlled launcher. Additionally, concerning the 10° cone constraint, it took about 3 days for ITASAT to settle down after injection in Case *II*, whereas it took up to 9 days in Case *I*. The ACS's settling time might be considered excessive when compared to, for instance, Holden *et al.* (1999). However, caution should be exerted when comparing with a much smaller satellite with much stronger magnetotorquers to exclusively dampen the nutation angle. Concerning Orlando *et al.* (1998) and Kuga *et al.* (1999), and the SCD-2's ACS design that inspired ITASAT's autonomous 3-axis attitude estimation and control system, passive nutation damping and a 10° dead-zone about the ecliptic plane normal were employed in SCD-2 to ultimately reach a 2.5° spin-axis pointing accuracy with respect to the ecliptic plane normal, and spin rate within $34 \pm 2\text{rpm}$. Since spin-axis pointing accuracy and spin rate are crucial for proper operation of the various on-board subsystems, mainly power and heat dissipation, the above results are of utmost importance to the mission analysis team. An integrated analysis of the joint ACS and heat dissipation for the purpose of thermal control is deemed mandatory to properly assess risks to mission success caused by the occasional trespassing of the 10° cone constraint during ITASAT's initial acquisition maneuver.

Thus, though pending further simulation of ITASAT's integrated ACS and heat dissipation subsystem, the results so far indicate a promising performance for ITASAT's ACS and make clear its correlation with the known, flight-tested SCD-2's ACS performance. Furthermore, the proposed ITASAT's ACS design showed robustness to a wide range of initial conditions that arise due to uncertainty whether the piggyback ride into the target orbit and injection will occur in a launcher with a spinning last stage, or 3-axis controlled. The results are also useful for the mission analysis team concerning the trade-off between ITASAT's ACS performance in the present target orbit and the capacity of the on-board battery powering the ACS prior to acquiring the proper attitude that enables battery charging via solar panel irradiation. Crucial to design decisions is the fact that ITASAT's ultimate target orbit is going to be that of the one, though yet unknown, primary payload that will fund the launch operation.

6. ACKNOWLEDGEMENTS

The authors acknowledge the funding support AEB/ITA/INPE ITASAT and FINEP/INPE/CTA Sistemas Inerciais para Aplicação Aeroespacial.

7. REFERENCES

- Alfriend, K. T., 1974, "Partially Filled Viscous Ring Nutation Damper", *J. Spacecraft*, Vol. 11, No 7, 1974.
- Azor, R., Bar-Itzhack, I. Y., Deutschmann, J. K. and Harman, R. R., 2001, "Angular-Rate Estimation Using Delayed Quaternion Measurements", *Journal of Guidance, Control, and Dynamics*, Vol. 24, No. 3, pp. 436-443.
- Carrara, V. and Guedes, U. T. V., 1994, "Attitude Control Aspects for SCD1 and SCD2", *Revista Brasileira de Ciências Mecânicas*, Vol. 16, pp. 83-87.
- Changsheng, Z., 2001, "Stability Analysis of Symmetrical Rotors Partially Filled with a Viscous Incompressible Fluid", *International Journal of Rotating Machinery*, Vol. 7, No. 5, pp. 301-310.

- Fonseca, I. M. and Souza, P.N., 1990, "Modelagem do Movimento Rotacional de um Corpo Rígido Dotado de um Amortecedor de Nutação Anular Viscoso e sua Validação Experimental", *Revista Brasileira de Ciências Mecânicas*, Vol. 12, No. 1, p. 89-111.
- Holden, T. E. and Lawrence, D. A., 1999, "A Lyapunov Design Approach to Magnetic Nutation Damping", *American Institute of Aeronautics and Astronautics – AIAA, Collection of Technical Papers*, Vol. 1, pp. 146-154.
- KROGH, K., 2002, "Attitude Determination for AAU CubeSat", M.Sc. dissertation, Aalborg University, Aalborg, Denmark.
- Kuga, H.K., Ferreira, L. D. D. and Guedes, U. T. V., 1987, "Simulação de Atitude e de Manobras para o Satélite Brasileiro Estabilizado por Rotação", *Proceedings of the 9th Brazilian Congress of Mechanical Engineering COBEM*, Florianópolis, SC.
- Kuga, H. K., Orlando, V. and Lopes, R. V. da F., 1999, "Flight Dynamics Operations During LEOP for INPE's Second Environmental Data Collecting Satellite SCD2", *Revista Brasileira de Ciências Mecânicas – Journal of the Brazilian Society of Mechanical Sciences*, Vol. 21, Special Issue, pp. 339-344.
- Lopes, R.V. da F.; Ricci, M.C. and Guedes, U.T.V., 1986, "Partially Filled Viscous Ring Nutation Damper: Brief Description and Preliminary Design", INPE Technical Report NTI-AMNUT-007-DMC/86 (in Portuguese).
- Lopes, R.V. da F., 1987, "Modelagem de um Amortecedor de Nutação para Satélites Estabilizados por Rotação", *Proceedings of the 9th Brazilian Congress of Mechanical Engineering COBEM*, Florianópolis, SC, pp. 761-764.
- Markley, F. L. and Sedlak, J. E., 2008, "Kalman Filter for Spinning Spacecraft Attitude Estimation", *Journal of Guidance, Control, and Dynamics*, Vol. 31, No. 6, pp.1750-1760.
- McLean, S., MacMillan, S., Maus, S., Lesur, V., Thomson, A., and Dater, D., 2004, "US/UK World Magnetic Model for 2005-2010", NOAA Technical Report NESDIS/NGDC-1.
- Orlando, V., Kuga, H. K. and Guedes, U. T. V., 1998, "Flight Dynamics LEOP and Routine Operations for SCD2, the Second Environmental Data Collecting Satellite", *American Astronautical Society*, Vol. 100, pp. 1003-1013.
- Santoni, F. and Tortoraf, P., 2000, "Magnetic Attitude Determination and Control of Small Spinning Spacecraft", *American Institute of Aeronautics and Astronautics – AIAA, Astrodynamics Specialist Conference*, Denver, CO, pp. 397-406.
- Santos, D. A., 2008, "Estimação de Atitude e Velocidade Angular de Satélites Utilizando Medidas do Campo Geomagnético e da Direção do Sol", M.Sc. dissertation, Instituto Tecnológico de Aeronáutica – ITA, São José dos Campos, SP.
- Santos, D. A. and Waldmann, J., 2008, "Attitude and Angular Rate Estimation from Vector Measurements of Magnetometer and Sun Sensor for a Low-Cost Satellite", submitted to 20th COBEM.
- Shigehara, M., 1972, "Geomagnetic Attitude Control of an Axisymmetric Spinning Satellite", *J. Spacecraft*, Vol. 9, No 6, 1972.
- Svartveit, K., 2003, "Attitude determination of the NCUBE satellite", M.Sc. dissertation, Norges Teknisk-Naturvitenskapelige Universitet, Trondheim.
- Vallado, D. A.; Crawford, P., Hujsak, R and Kelso, T. S., 2006, "Revisiting Spacetrack Report #3", *American Institute of Aeronautics and Astronautics – AIAA, Astrodynamics Specialist Conference and Exhibit*, Keystone, Colorado.
- Vreeburg, J. P.B., 2005, "Spacecraft Maneuvers and SLOSH Control", *IEEE Control Systems Magazine*, Vol. 25, No. 3, June, pp. 12-16.
- Waschburger, R., Viana, I. B., Nepomuceno, A. L. and Waldmann, J., 2008a, "Simulação do Sistema de Controle de Atitude do Satélite Universitário Itasat para Avaliação da Viabilidade de Atuação Puramente Magnética", *Proceedings of the 5th Congresso Nacional de Engenharia Mecânica - CONEM*, BA.
- Waschburger, R. and Waldmann, J., 2008b, "Critérios para Ativação dos Magnetotorqueadores em Sistema de Controle de Atitude com Atuação Puramente Magnética do Satélite Universitário ITASAT", *Proceedings of the Congresso Brasileiro de Automática - CBA*, Juiz de Fora - MG.
- Wertz, J. (ed.), 1978, "Spacecraft Attitude Determination and Control", The Netherlands: Kluwer Academic Publishers.
- Wiesel, W. E., 1977, "Spaceflight Dynamics", 2nd. Ed., McGraw-Hill.
- Wisniewski, R., 2000, "Linear Time Varying Approach to Satellite Attitude Control Using Only Electromagnetic Actuation", *Journal of Guidance, Control, and Dynamics*, Vol. 23, No. 4, pp. 640-647.
- Zanardi, M. C. and LOPES, R. V. da F., 2000, "Space Attitude Representation, Propagation and Determination: Theory and Some Applications on the Brazilian Space Program", *Advances in Space Dynamics*, pp. 503-515.

8. RESPONSIBILITY NOTICE

The authors are the only responsible for the printed material included in this paper.